Efthymios S. Folias[1]

Some Remarks on Three-Dimensional Fracture

REFERENCE: Folias, E. S., **"Some Remarks on Three-Dimensional Fracture,"** *Fracture Mechanics: Nineteenth Symposium, ASTM STP 969,* T. A. Cruse, Ed., American Society for Testing and Materials, Philadelphia, 1988, pp. 56–72.

ABSTRACT: In this paper, the author presents the effect of specimen thickness on the stress concentration factor of a plate that has been weakened by a circular hole. The results compare very well with existing results on thin and very thick plates and bridge the data gap between them. Furthermore, the solution is shown to be derived from the same general solution from which the three-dimensional crack problem solution can be derived. The author also, by analogy, draws some conclusions regarding the behavior of the stress intensity factor.

KEY WORDS: thickness effect, stress concentration factor, circular hole, three-dimensional analysis, fracture, fracture mechanics

In the field of fracture mechanics it is well recognized that the role which the specimen thickness plays in the mechanism of failure is not very well understood. For example, the common experimental observation of a change from ductile failure at the edge to brittle fracture at the center of a broken sheet material has so far defied analysis. Moreover, the fracture toughness of a material is assumed to be constant. Yet failure theories in the field of fracture mechanics define two different values for fracture toughness, K_c and K_{Ic}.

Similarly, the failure of linear elastic fracture mechanics (LEFM) to predict the behavior of short cracks to the same degree of accuracy as that obtained for long crack behavior is usually attributed to one of two reasons (or possibly both). These are either that LEFM is not the appropriate analysis technique, or that other effects not normally accounted for are important and must be included.

Factors which are often neglected in LEFM analysis, but which are likely to be important in short crack conditions, fall into three categories:

(*a*) surface conditions (for example, residual stresses due to machining, cold working, or chemical finishing, and applied stresses due to fretting),
(*b*) three-dimensional considerations, and
(*c*) plasticity considerations (for example, a yielded zone at the crack tip and also crack closure due to the wake of the yielded material).

While undoubtedly all three categories are equally important for the proper understanding of short crack growth behavior, the author believes that it is rather premature for researchers to conclude that LEFM theories do not adequately predict the behavior of short cracks and that considerations of realistic, three-dimensional, specimen geometries becomes ever more essential. Thus, an orderly theoretical attack on the three-dimensional Griffith problem can provide guidance to these and other phases of fracture research.

The most potent mathematical tool for this attack is the linear theory of infinitesimal

[1] Professor, University of Utah, Department of Civil Engineering, Salt Lake City, UT 84112.

elasticity as applied to a cracked plate of finite thickness. While it is true that this theory cannot include the nonelastic behavior of the material at the crack tip per se, it can (1) show many characteristics of the actual behavior of a cracked plate, including those due to thickness, and (2) assist us in understanding better the three-dimensional elastic-plastic analog (for example, by providing us with a proper discretized element mesh). Thus, the theory of three-dimensional linear elasticity is a logical fountainhead for detailed theoretical study, for it represents a relatively simple mathematical model.

Even so, the mathematical difficulties posed by three-dimensional problems are substantially greater than those associated with either plane stress or plane strain. As a result, there exist in the literature very few analytical papers[2] that deal specifically with the three-dimensional stress character at the base of a stationary crack. Simultaneously, in the last two decades, numerous attempts have been made to obtain finite element solutions by very capable researchers. Although they, too, have experienced some difficulties in the past,[3] at present a consensus appears to have emerged as will be evident from the results presented in this volume. The fact, however, remains that there exists no explicit analytical solution with which numerical results can be compared. Be that as it may, the following three-dimensional elasticity problems immediately come to mind:

(*a*) a plate weakened by a cylindrical hole,
(*b*) a plate weakened by a through crack, and
(*c*) a plate weakened by a partially through crack,

listed in the order of relative difficulty.

In this paper, the author will present some numerical results for the first problem and, by analogy, draw certain conclusions for the second problem. Moreover, the results of the first problem will be compared with two existing asymptotic solutions, one applicable to thin plates and the other applicable to very thick plates. The main purpose of this paper, however, is threefold: first, to show that the solution of the cylindrical hole problem is derivable from the same general analytical solution that the three-dimensional crack problem solution can be derived from; second, to acquire enough experience and a "feel" for the ultimate construction of an explicit analytical solution to the crack problem; and, third, to illustrate how the general solution for the equilibrium of elastic layers can be used effectively to solve a whole class of three-dimensional problems of practical interest.

Effect of Thickness

A general three-dimensional solution to Navier's equation for plates of uniform thickness, $2h$, and with plate faces free of stress has previously been constructed by the author, and the results are reported in Ref *2*. Perhaps it may be appropriate here to note that the same displacement field is also recovered if one uses a double Fourier integral transform in x and y and, subsequently, a contour integration. This matter is discussed in great detail in Ref *3*. Without going into the mathematical details, the general displacement field can be found in the Appendix where it has been written in a more convenient form.

By choosing appropriately the remaining five arbitrary functions, that is, H_v, H_n^*, I_1, I_2, and I_3, one may now solve a whole class of three-dimensional linear elastic problems, for example, the problem of a cylindrical hole, an elliptical hole, a crack, a cylindrical inclusion,

[2] For a historical discussion see Ref *1*.

[3] See *Proceedings,* Workshop on Three-Dimensional Fracture Analysis, held at Battelle, Columbus, OH, 26–28 April 1976.

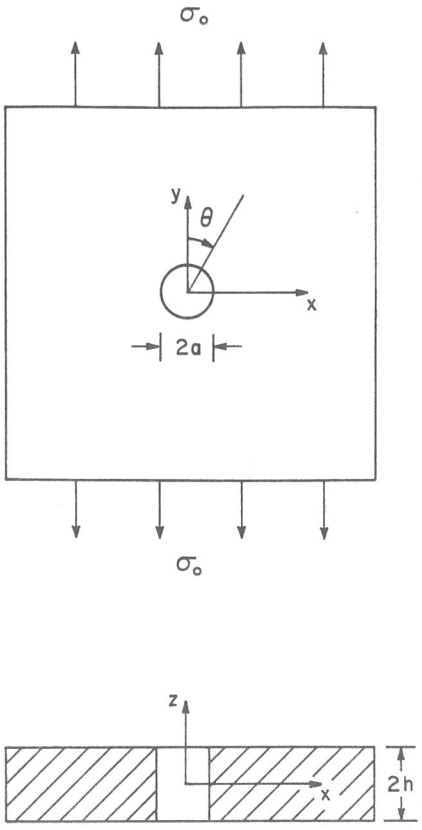

FIG. 1—*Geometrical configuration of a plate weakened by a circular hole of radius* a.

and so forth. In Ref *4*, for example, the author uses the problem of a plate weakened by a cylindrical hole (see Fig. 1) as a vehicle to show how the general solution can be used to construct the three-dimensional stress field. The problem was ultimately reduced to the solution of three equations involving a series of complex eigenfunctions for the determination of the unknown, but constant, coefficients. These equations represent the free-of-stress boundary conditions at the surface of the hole where the θ and r dependence has now been totally eliminated.

Without going into the mathematical details, the system was solved numerically,[4] and the stress concentration factor at $\theta = \pi/2$ and $r = a$ was computed for various radius-to-thickness ratios, a/h, and for Poisson's ratio of $\nu = 0.33$. The results are presented in Figs. 2 through 7. It may be noted that double precision was used throughout the numerical work and that a very sophisticated algorithm was used for the evaluation of the Bessel modified functions of the second kind.

The results show the stress concentration factor to be sensitive to the ratio of (a/h) and to Poisson's ratio ν. For example, for $\nu = 0.33$ and ratios of $(a/h) \geq 0.5$, it was found that the stress concentration factor attains its maximum in the middle of the plate and decreases parabolically as one approaches the free surfaces. On the other hand, for $(a/h) < 0.5$, the

[4] It should be noted that we have also constructed the orthogonality condition of these eigenfunctions.

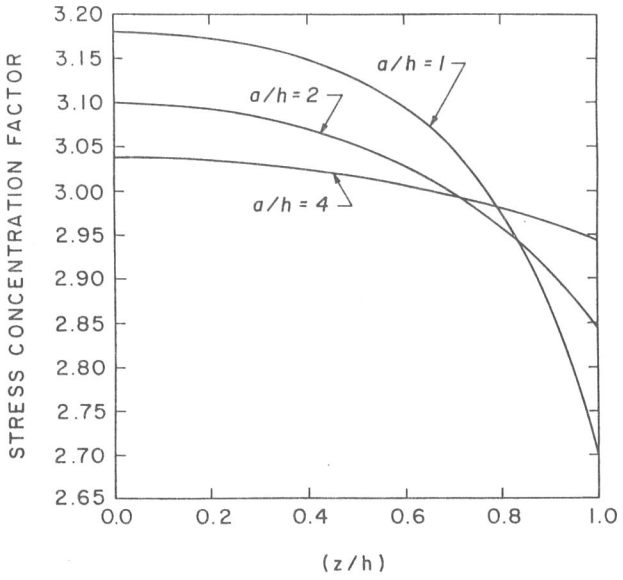

FIG. 2—*Stress concentration factor across the thickness for Poisson's ratio* $\nu = 0.33$ *and various* a/h *ratios.*

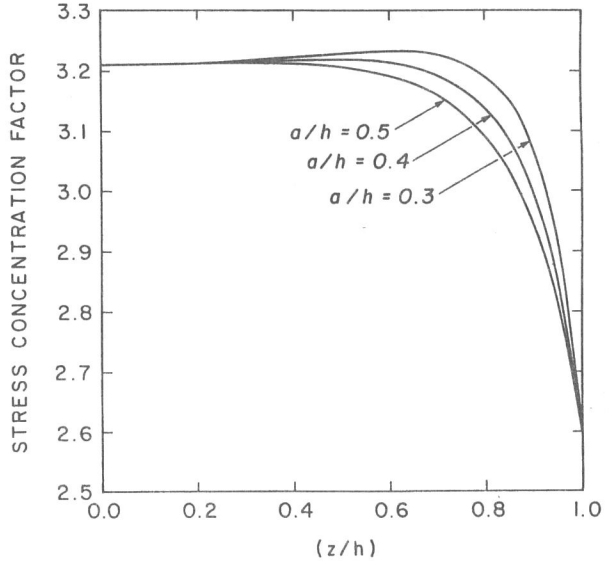

FIG. 3—*Stress concentration factor across the thickness for Poisson's ratio* $\nu = 0.33$ *and various* a/h *ratios.*

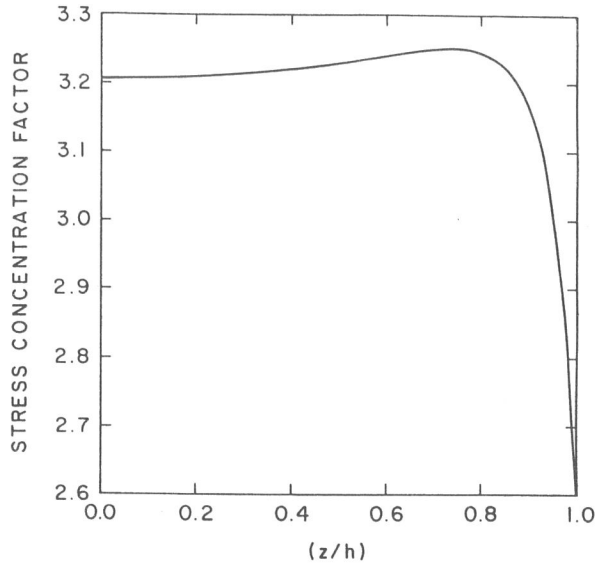

FIG. 4—*Stress concentration factor across the thickness for Poisson's ratio of* $\nu = 0.33$ *and* a/h = *0.2.*

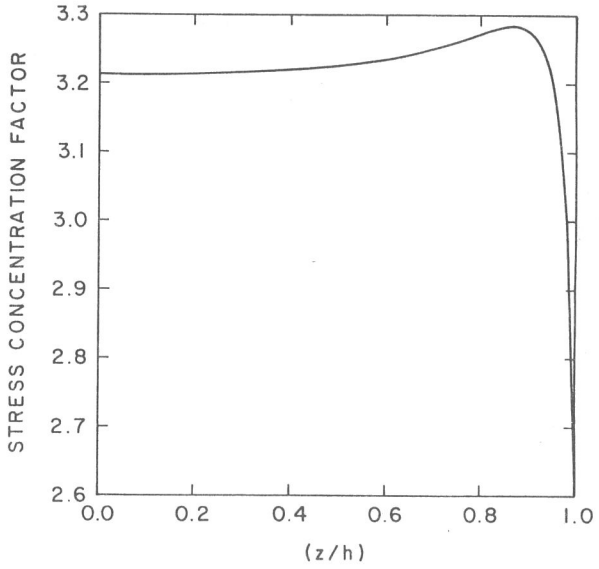

FIG. 5—*Stress concentration factor across the thickness for Poisson's ratio of* $\nu = 0.33$ *and* a/h = *0.1.*

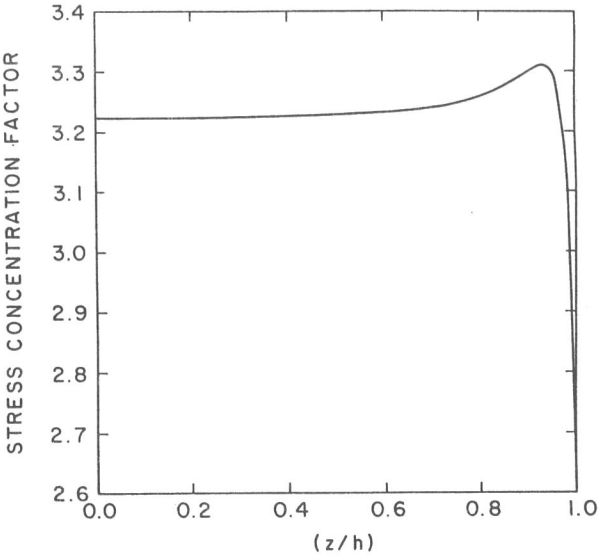

FIG. 6—*Stress concentration factor across the thickness for Poisson's ratio of* $\nu = 0.33$ *and* a/h = *0.05.*

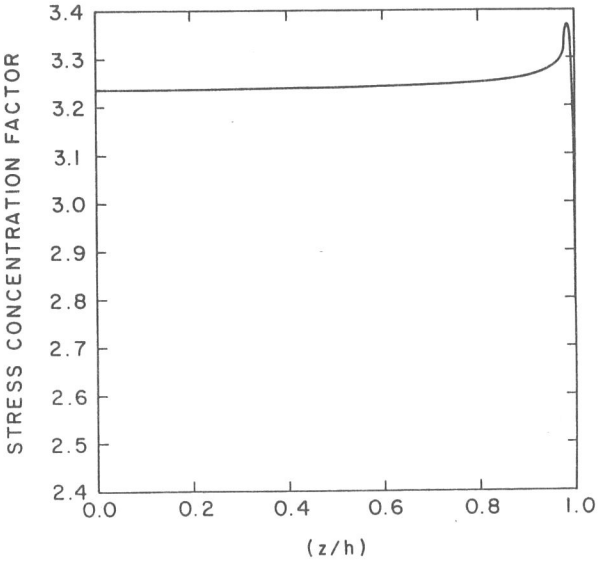

FIG. 7—*Stress concentration factor across the thickness for Poisson's ratio of* $\nu = 0.33$ *and* a/h = *0.01.*

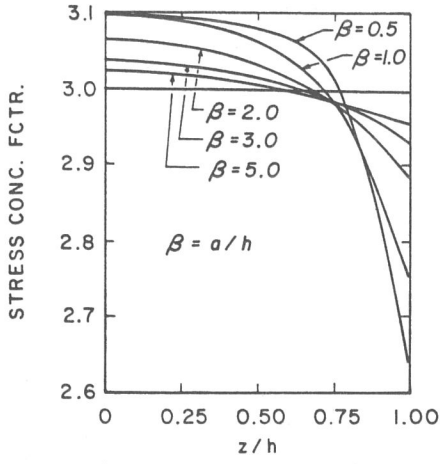

FIG. 8—*Stress concentration factor across the thickness for Poisson's ratio* $\nu = 0.25$ *and various* a/h *ratios (Alblas 1957).*

stress concentration factor attains its maximum close to the plate faces. Moreover, as the ratio of a/h decreases further, the following numerical trends are observed for the stress concentration factor (SCF):

(a) the magnitude of the rise slowly increases,[5]
(b) the maximum occurs closer and closer to the free surface so that the depth below the surface approaches the radius of the hole,
(c) at the surface of the plate it drops rather abruptly, and
(d) the magnitude at the surface slowly decreases.

It is appropriate at this time to compare our results with those already existing in the literature. Historically, the two-dimensional problem was first studied by Kirsch [*5*] in 1898 and the stress concentration factor was found to be equal to three. It was not until 1948 that Green [*6*] constructed a three-dimensional solution which was in an infinite series form. Unfortunately, he did not pursue the solution far enough to extract numerical results. In 1949, Sternberg and Sadowsky [*7*] used a modified version of the Ritz method to obtain an approximate solution to the problem. Subsequently, in 1957 Alblas [*8*], applying the same scheme proposed by Green, succeeded in obtaining a solution in a more convenient series from whereby he was able to perform extensive numerical calculations. His results for Poisson's ratio of $\nu = 1/4$ are shown in Fig. 8. For ratios of $(a/h) > 1$ our results are identical to those obtained by Alblas. Moreover, for the ratio of $(a/h) = 1$ the difference is minimal, as can be seen by a comparison of the results in Fig. 9. The small difference is attributed to the fact that Alblas at that time did not have access to modern computer facilities; consequently, he was forced to truncate the system to 14 roots.

Our results on the other hand, reflect the use of 300 roots. Even so, the agreement for ratios of $(a/h) \geq 1$ is remarkably good. For ratios of $(a/h) < 1$, however, more roots are needed to eliminate undesirable oscillations, and therefore he was forced to limit his calculation to ratios of $(a/h) \geq 0.5$.

[5] The reader should be cautioned that this remark does not necessarily imply that the SCF will increase indefinitely.

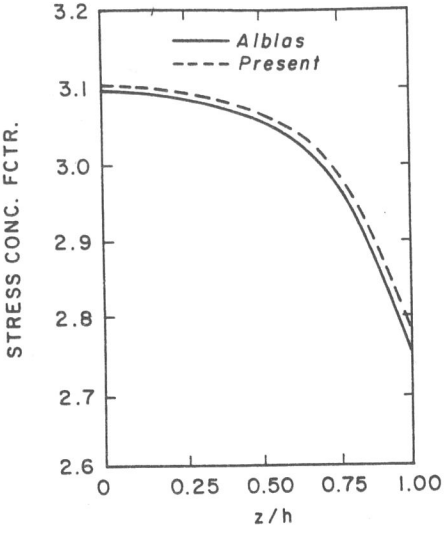

FIG. 9—*Comparison of the stress concentration factor for* $\nu = 0.25$ *and* a/h $= 1.0$.

In 1962, Reiss [*9*] using a perturbation analysis was able to obtain a solution which yielded "three-dimensional" corrections to those of the generalized plane stress. The results are shown in Fig. 10. Finally, in 1966 Youngdahl and Sternberg [*10*], recognizing the sensitivity of the SCF on the diameter-to-thickness ratio, studied the problem of a half-space with a hole in order to establish the behavior of the SCF for very thick plates. The problem was finally casted into a Fredholm integral equation of the second kind, the solution of which was finally sought numerically. Perhaps it is appropriate at this point to state an observation made by the authors of Ref *10*:

> the burden of the numerical analysis of the solution established was at least equal to the effort expended on its derivation.

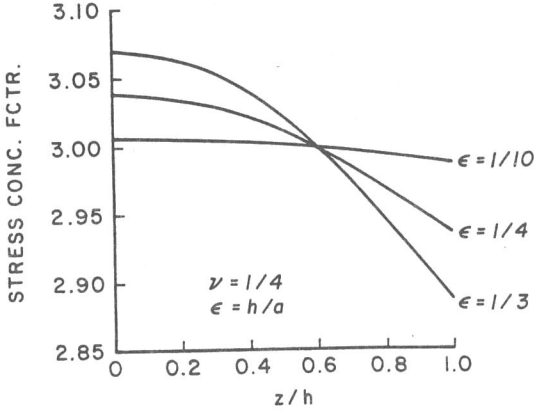

FIG. 10—*Stress concentration factor across the thickness for Poisson's ratio* $\nu = 0.25$ *and various* a/h *ratios (Reiss 1963).*

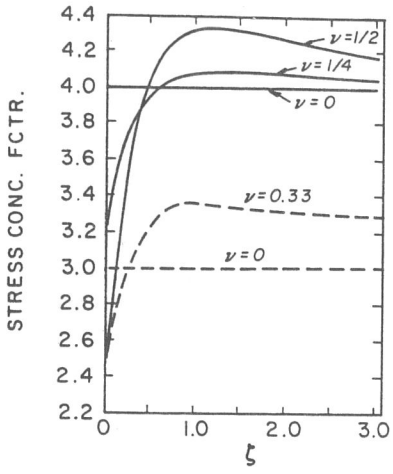

FIG. 11—*Comparison of the stress concentration factor in the vicinity of the free surface with results of Ref* 10.

The present author also concurs with this observation, for the nature of this problem is such that it does not lend itself to routine numerical calculations.

In any event, their results clearly show the existence of a three-dimensional stress boundary layer that emerges near the edges of the hole in the analogous problem of a plate of finite thickness, as the ratio of the diameter of the hole to the plate thickness becomes very small. Our present results substantiate the existence of such a boundary layer at the vicinity of the free surfaces. In fact, if we examine the local behavior of the rise, for example, for the ratio of $(a/h) = 0.01$, and stretch the variable by letting $\zeta = 100(1 - z/h)$, we observe (see Fig. 11) that the behavior is similar to[6] that obtained by Youngdahl and Sternberg [*10*]. We also observe that the rise here is not quite as noticeable as in Fig. 7. This is due to the vertical scale, which the authors of Ref *10* used, and to the stretching of the horizontal variable z/h. In view of the findings of Ref *10*, one concludes that the surface effects become dominant and that the amplitude of the characteristic rise ultimately reaches an upper bound.[7] This matter will be investigated further in the section on stress behavior at the corner.

Finally, it is appropriate to comment on the conditions of plane stress and plane strain. For $(a/h) \to \infty$, our numerical results give precisely the value of plane stress, that is, the value of three. Similarly, for $\nu = 0$ the value of three is also recovered. This result meets our expectations, for it represents an exact solution.

In the case of plane strain, the boundary planes $z = \pm h$ are thrown to infinity, and simultaneously the boundary conditions must be relaxed by requiring that all stresses and displacements must be finite. Assuming that the radius of the hole is sufficiently large, the author suspects that the SCF at the center of the plate will begin to slowly decrease as the ratio of a/h decreases beyond the value of 0.01, until it finally reaches the value of plane strain. Such an effort, however, requires considerably more computer time than was available to us.

[6] In Ref *10*, the reader should notice that the loading is in both the x and y directions.

[7] For $a/h = 0.01$ and $\nu = 0.33$, our numerical results show the max value of the SCF to be 3.3675. This value should be very close to the upper bound. It is interesting to note that it is $\approx 3/(1 - \nu^2)$.

Observations On Some Numerical Results

Before we attempt to interpret the physical meaning of the numerical results, particularly at the neighborhood of the intersection between the hole and the free surface, it will be appropriate for us first to examine the numerical results of a well known two-dimensional solution and then, we hope, to make some associations.

Let us consider for the sake of discussion the two curves, I and J, shown on Fig. 12. The curves have been drawn based on a number of calculated points which, for convenience, have been located on the graphs. Furthermore, let us assume that these curves represent the two local stress profiles τ_{xz} and σ_{xx}, respectively, in a body that lies to the right of the vertical axis, has the vertical axis as a boundary, and is symmetric with respect to the z-axis. The stress profiles have been calculated along the line $x = 0.05$. Given this limited information, can one draw a definite conclusion as to whether or not a stress singularity exists at the point $x = z = 0$?

An examination of the stress curves shows that, as one moves from right to left along the line $x = 0.05$, both stresses are initially zero, then rise slowly to reach a maximum, and finally decrease to zero as the value of $z = 0$ is reached. Because the stress drops as one approaches the boundary, one is tempted to conclude that there exists no stress singularity at the point $x = z = 0$. But this would be an erroneous conclusion since this particular stress field represents that of a concentrated line load P on a half space (see Fig. 13), that is

$$\tau_{xz} = -\frac{2P}{\pi r}\sin\phi\cos^2\phi = -\frac{2P}{\pi}\frac{xz^2}{(x^2+z^2)^2} = -PI$$

$$\sigma_{xx} = -\frac{2P}{\pi r}\cos\phi\sin^2\phi = -\frac{2P}{\pi}\frac{x^2z}{(x^2+z^2)^2} = -PJ$$

$$\sigma_{zz} = -\frac{2P}{\pi r}\cos^3\phi$$

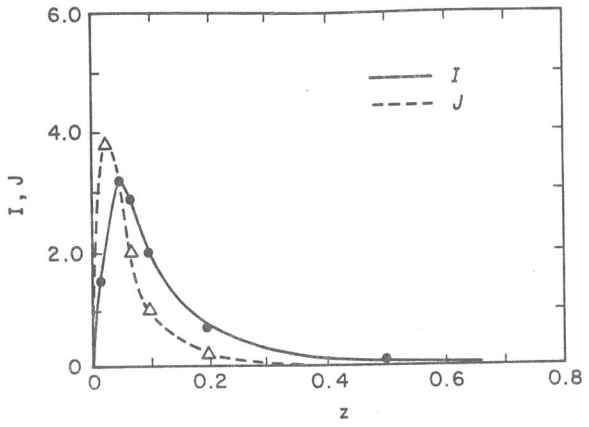

FIG. 12—*The functions* I *and* J *for* x = *0.05 and various values of* z.

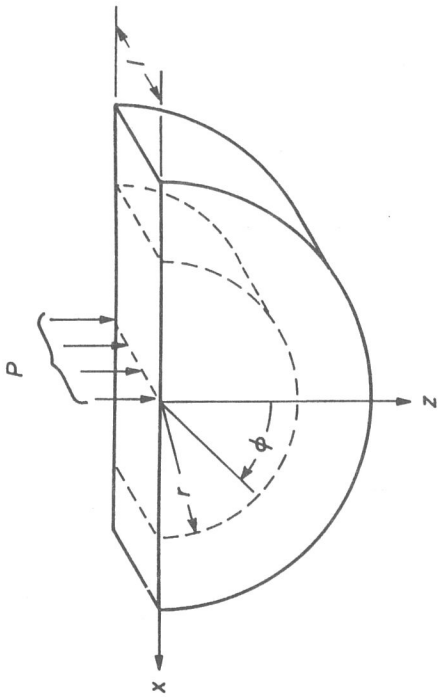

FIG. 13—*Geometrical configuration.*

where ϕ now represents the angle from the horizontal axis. By examining the above equations more carefully, we notice that the location of the maximum rise depends on the chosen value of x. In particular, I and J attain their maximums at $z = x$ and $z = x/\sqrt{3}$, respectively. This suggests, therefore, that as the value of x becomes smaller and smaller, the rise moves closer and closer to the x-axis while its amplitude increases simultaneously. Furthermore, it should be noted that for a given value of x, similar stress profiles are observed. In view of the above, the author makes the following observations:

1. As one approaches the free surface, the stresses exhibit a rise or a hump.
2. At the surface, the stresses decrease rather abruptly to zero.
3. As x decreases, the amplitude of the rise increases.
4. The analytical solution exhibits the presence of a stress singularity at $x = z = 0$.

Let us next look at another related problem which was studied[8] by Filon in 1903. He discusses the case shown in Fig. 14*a*, where the forces P are displaced one with respect to the other. The distribution of shearing stresses over the cross section *nn* in this case is shown in Fig. 14*b*. Notice that for small values of the ratio b/c this distribution does not resemble the parabolic distribution given by the elementary theory, and that there are very large stresses at the top and bottom of the beam while the middle portion of the beam is practically free from shearing stresses. One conjectures, therefore, that close to the free surfaces there exists a boundary layer solution. Moreover, we know that at the point of application of the load there exists a stress singularity, the presence of which is not evident from the numerical

[8] See also Timoshenko and Goodier, *Theory of Elasticity*, 3rd ed., pp. 57–58.

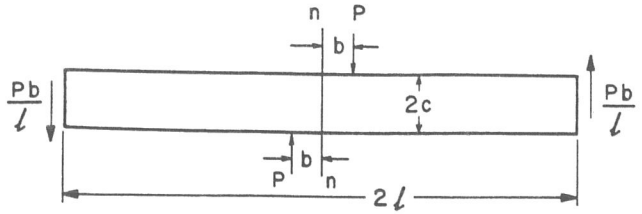

FIG. 14*a*—*Geometrical configuration of a beam subjected to two concentrated loads.*

work depicted in Fig. 14*b*. In fact, the numerical results show the shear stress there to vanish.

It becomes evident from this discussion that even though the numerical results show the stress profiles to vanish at the boundary, this does not necessarily exclude the possiblity of a stress singularity being present at certain points of the boundary.

The Stress Behavior at the Corner

Finally it is of some academic and practical interest to examine the behavior of the stress field in the very immediate vicinity of the corner point, that is, the point where the hole meets the free surface of the plate. However, in view of our previous discussion, such information is best if it is extracted by analytical rather than numerical means. Utilizing the local coordinates of the corner point, an asymptotic analysis was carried out for the exponent α of an assumed displacement field $u_i \sim \rho^{\alpha}$, where $\rho \ll a$. Without going into the mathematical details, the satisfaction of all the boundary conditions of the three-dimensional stress problem

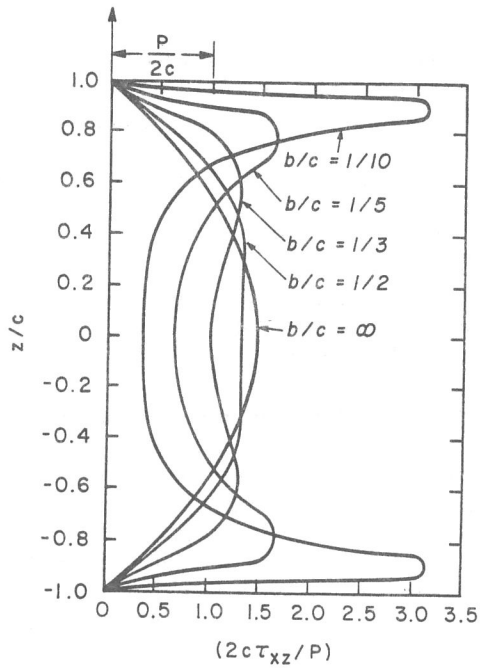

FIG. 14*b*—*The behavior of the shear stress over the Cross Section* n-n *for various ratios of* b/c.

lead to a characteristic equation which has an infinite number of complex roots. It is interesting to note that the first root is the same as that obtained by the Williams solution [*11*] for a 90° corner with free free-of-stress boundaries, that is, $\alpha = 2.739\ 59 \pm 1.119\ 02$. While this result was to be anticipated on intuitive grounds, it could not be taken for granted. The details of this asymptotic analysis will be reported in a future paper.

In view of the above, one may draw the following conclusions:

1. The solution is derivable from a general three-dimensional solution to Navier's equations.
2. The solution recovers the existing limiting results for thin plates [*8,9*] as well as for thick plates [*10*] and bridges the gap between them.
3. For ratios of $(a/h) \geq 0.5$, the maximum stress occurs in the middle plane.
4. For ratios of $(a/h) < 0.5$, the maximum stress occurs close to the free surface (approximately one radius distance away from the surface).
5. The results show the transition between thin and thick plates to occur at a ratio of $(a/h) = 0.5$.
6. As a/h becomes small, there exists in the neighborhood of the free surfaces a boundary layer solution similar to that reported in Ref *10*.
7. Depending on the value of the ratio of a/h, the fatigue life of the member may be substantially shorter than that predicted by the two-dimensional elasticity theory.
8. For $\rho \ll a$, there is no stress singularity present at the corner where the hole intersects the free surface of the plate.

The Crack Problem

Inasmuch as the solution of both the hole and the crack problems can be obtained from the same general three-dimensional solution, similar trends are expected to prevail. Therefore, by analogy, one is tempted to conclude the following regarding the stress intensity factor:

1. It will be sensitive to the crack-to-thickness ratio and to Poisson's ratio, ν.
2. It will drop rather abruptly at the free surface.
3. For certain values of c/h, it will attain a maximum at the middle plane and will decrease parabolically as one approaches the free surface.
4. For the remaining values of c/h, the maximum will occur closer to the free surface (approximately half a crack size away), where a small rise will develop.
5. For relatively thick plates, the shear lip will be found to be related to the width of this rise.
6. No conclusion can be drawn from this analysis regarding the corner singularity.

Engineering fracture mechanics can deliver the methodology to compensate for the inadequacies of conventional design concepts that were based on tensile strength or yield strength. While such criteria are adequate for many engineering structures, they are insufficient when the likelihood of cracks exists. Now, after approximately three decades of development, fracture mechanics has become a useful tool in design, particularly with high-strength materials. Interestingly enough, this advancement has been based primarily on the two-dimensional solution of the Griffith crack problem. We believe that the three-dimensional solution of the Griffith crack problem will not only enable us to understand the mechanism of fracture propagation better, but it will also expand our horizons for future

research and, we hope, will contribute to the advancement of the field of fracture mechanics to higher levels of safe design against fracture.

Acknowledgment

The contents of this paper are an outgrowth of some previous work on three-dimensional fracture which was supported by the U.S. Air Force Office of Scientific Research. The author is grateful for this support.

APPENDIX

A general solution to Navier's equations for plates of uniform thickness, $2h$, and with the plate faces free of stress has already been constructed by the author and the results are reported in Ref *2*. Thus, without going into the long and tedious mathematical details, the complementary displacement and stress fields may be written in the form:

The Displacement Field

$$u^{(c)} = \frac{1}{m-2}\sum_{\nu=1}^{\infty} A_\nu \frac{\partial H_\nu}{\partial x}\,[2(m-1)\cos(\beta_\nu h)\cos(\beta_\nu z)$$

$$+ m\beta_\nu h \sin(\beta_\nu h)\cos(\beta_\nu z) - m\beta_\nu z\cos(\beta_\nu h)\sin(\beta_\nu z)]$$

$$+ \sum_{n=1}^{\infty} B_n \frac{\partial H_n^*}{\partial y}\cos(\alpha_n h)\cos(\alpha_n z)$$

$$+ I_1 - y\frac{\partial I_3}{\partial x} + \frac{1}{m+1} z^2 \frac{\partial^2 I_3}{\partial x \partial y}$$

$$v^{(c)} = \frac{1}{m-2}\sum_{\nu=1}^{\infty} A_\nu \frac{\partial H_\nu}{\partial y}\,[2(m-1)\cos(\beta_\nu h)\cos(\beta_\nu z)$$

$$+ m\beta_\nu h \sin(\beta_\nu h)\cos(\beta_\nu z) - m\beta_\nu z\cos(\beta_\nu h)\sin(\beta_\nu z)]$$

$$- \sum_{n=1}^{\infty} B_n \frac{\partial H_n^*}{\partial x}\cos(\alpha_n h)\cos(\alpha_n z) + \frac{3m-1}{m+1} I_3 + I_2$$

$$- y\frac{\partial I_3}{\partial y} - \frac{1}{m+1} z^2 \frac{\partial^2 I_3}{\partial x^2}$$

$$w^{(c)} = \frac{1}{m-2}\sum_{\nu=1}^{\infty} A_\nu H_\nu \beta_\nu [(m-2)\cos(\beta_\nu h)\sin(\beta_\nu z)$$

$$- m\beta_\nu h \sin(\beta_\nu h)\sin(\beta_\nu z) - m\beta_\nu z\cos(\beta_\nu h)\cos(\beta_\nu z)]$$

$$- \frac{2}{m+1} z \frac{\partial I_3}{\partial y}$$

The Stress Field

$$\frac{1}{2G}\sigma_{xx}^{(c)} = \frac{2}{m-2}\sum_{\nu=1}^{\infty} A_\nu \beta_\nu^2 H_\nu \cos(\beta_\nu h)\cos(\beta_\nu z)$$

$$+ \frac{1}{m-2}\sum_{\nu=1}^{\infty} A_\nu \frac{\partial^2 H_\nu}{\partial x^2}[2(m-1)\cos(\beta_\nu h)\cos(\beta_\nu z)$$

$$+ m\beta_\nu h \sin(\beta_\nu h)\cos(\beta_\nu z) - m\beta_\nu z \cos(\beta_n h)\sin(\beta_\nu z)]$$

$$+ \sum_{n=1}^{\infty} B_n \frac{\partial^2 H_n^*}{\partial x \partial y}\cos(\alpha_n h)\cos(\alpha_n z)$$

$$+ \frac{\partial I_1}{\partial x} - y\frac{\partial^2 I_3}{\partial x^2} + \frac{1}{m+1}z^2\frac{\partial^3 I_3}{\partial x^2 \partial y} + \frac{2}{m+1}\frac{\partial I_3}{\partial y}$$

$$\frac{1}{2G}\sigma_{yy}^{(c)} = \frac{2}{m-2}\sum_{\nu=1}^{\infty} \beta_\nu^2 A_\nu H_\nu \cos(\beta_\nu h)\cos(\beta_\nu z)$$

$$- \frac{1}{m-2}\sum_{\nu=1}^{\infty} A_\nu \left[\frac{\partial^2 H_\nu}{\partial x^2} - \beta_\nu^2 H_\nu\right][2(m-1)\cos(\beta_\nu h)\cos(\beta_\nu z)$$

$$+ m\beta_\nu h \sin(\beta_\nu h)\cos(\beta_\nu z) - m\beta_\nu z \cos(\beta_\nu h)\sin(\beta_\nu z)]$$

$$- \sum_{n=1}^{\infty} B_n \frac{\partial^2 H_n^*}{\partial x \partial y}\cos(\alpha_n h)\cos(\alpha_n z)$$

$$+ \frac{2m}{m+1}\frac{\partial I_3}{\partial y} - \frac{\partial I_1}{\partial x} + y\frac{\partial^2 I_3}{\partial x^2} - \frac{1}{m+1}z^2\frac{\partial^3 I_3}{\partial x^2 \partial y}$$

$$\frac{1}{2G}\sigma_{zz}^{(c)} = \frac{m}{m-2}\sum_{\nu=1}^{\infty} A_\nu H_\nu \beta_\nu^2[-\beta_\nu h \sin(\beta_\nu h)\cos(\beta_\nu z)$$

$$+ \beta_\nu z \cos(\beta_\nu h)\sin(\beta_\nu z)]$$

$$\frac{1}{G}\tau_{xy}^{(c)} = \frac{2}{m-2}\sum_{\nu=1}^{\infty} A_\nu \frac{\partial^2 H_\nu}{\partial x \partial y}[2(m-1)\cos(\beta_\nu h)\cos(\beta_\nu z)$$

$$+ m\beta_\nu h \sin(\beta_\nu h)\cos(\beta_\nu z) - m\beta_\nu z \cos(\beta_\nu h)\sin(\beta_\nu z)]$$

$$- \sum_{n=1}^{\infty} B_n \left[2\frac{\partial^2 H_n^*}{\partial x^2} - \alpha_n^2 H_n^*\right]\cos(\alpha_n h)\cos(\alpha_n z)$$

$$+ 2\left(\frac{m-1}{m+1}\right)\frac{\partial I_3}{\partial x} + 2\frac{\partial I_2}{\partial x} - \frac{2}{m+1}z^2\frac{\partial^3 I_3}{\partial x^3} - 2y\frac{\partial^2 I_3}{\partial x \partial y}$$

$$\frac{1}{G}\tau_{xz}^{(c)} = -\frac{2m}{m-2}\sum_{\nu=1}^{\infty} A_\nu \frac{\partial H_\nu}{\partial x}\beta_\nu[\cos(\beta_\nu h)\sin(\beta_\nu z)$$

$$+ \beta_\nu h \sin(\beta_\nu h)\sin(\beta_\nu z) + \beta_\nu z \cos(\beta_\nu h)\cos(\beta_\nu z)]$$

$$- \sum_{n=1}^{\infty} B_n \frac{\partial H_n^*}{\partial y}\alpha_n \cos(\alpha_n h)\sin(\alpha_n z)$$

$$\frac{1}{G}\tau_{yz}^{(c)} = -\frac{2m}{m-2}\sum_{\nu=1}^{\infty} A_\nu\beta_\nu \frac{\partial H_\nu}{\partial y}[\cos(\beta_\nu h)\sin(\beta_\nu z)$$

$$+ \beta_\nu h \sin(\beta_\nu h)\sin(\beta_\nu z) + \beta_\nu z \cos(\beta_\nu h)\cos(\beta_\nu z)]$$

$$+ \sum_{n=1}^{\infty} B_n a_n \frac{\partial H_n^*}{\partial x}\cos(\alpha_n h)\sin(\alpha_n z)$$

where A_ν and B_n are functions of β_ν and α_n, respectively,

$$\alpha_n \equiv \frac{n\pi}{h} \qquad n = 1,2,3,\ldots,$$

β_ν are the roots of the transcendental equation

$$\sin(2\beta_\nu h) = -2(\beta_\nu h)$$

and the functions H_ν and H_n^* satisfy the reduced wave equation, that is,

$$\frac{\partial^2 H_\nu}{\partial x^2} + \frac{\partial^2 H_\nu}{\partial y^2} - \beta_\nu^2 H_\nu = 0$$

and

$$\frac{\partial^2 H_n^*}{\partial x^2} + \frac{\partial^2 H_n^*}{\partial y^2} - \alpha_n^2 H_n^* = 0$$

and I_1, I_2, and I_3 are two-dimensional harmonic functions such that

$$I_1 = Im\phi$$

$$I_2 = Re\phi$$

References

[1] Folias, E. S., *International Journal of Fracture,* Vol. 16, No. 4, August 1980, pp. 335–348.
[2] Folias, E. S., *Journal of Applied Mechanics,* Vol. 42, No. 3, September 1975, pp. 663–674.
[3] Wilcox, C. H., "Completeness of the Eigenfunctions for Griffith Cracks in Plates of Finite Thickness," Interim Report, Department of Mathematics, University of Utah, Salt Lake City, UT, December 1978.

[4] Folias, E. S. and Wang, J. J., "On the Three-Dimensional Stress Field Around a Circular Hole in a Plate of Arbitrary Thickness," College of Engineering Report, University of Utah, Salt Lake City, UT, January, 1985.
[5] Kirsch, G., *Zentralblatt verein Deutscher Ingenieure,* Vol. 42, 1898, p. 797.
[6] Green, A. E., *Transactions of the Royal Society of London, Series A,* Vol. 240.285, 1948, p. 561.
[7] Sternberg E. and Sadowsky, M. A., *Journal of Applied Mechanics,* Vol. 16, 1949, pp. 27–38.
[8] Alblas, J. B., "Theorie van de driedimensionle spanningstodestand in een doorboovde platt," Ph.D. dissertation, Technische Hogeschool Delft, Amsterdam, The Netherlands, 1957.
[9] Reiss, E. L., "Extension of an Infinite Plate with a Circular Hole, *Journal of the Society for Industrial and Applied Mathematics,* Vol. 11, No. 4, 1963, p. 840.
[10] Youngdahl, C. K. and Sternberg, E., *Journal of Applied Mechanics,* December 1966, pp. 855–865.
[11] Williams, M. L., *Journal of Applied Mechanics,* Vol. 19, 1952, p. 526.